JOURNAL OF VIROLOGY, Nov. 2009, p. 11201–11210 Vol. 83, No. 21
0022-538X/09/$12.00 doi:10.1128/JVI.01025-09

Extension of Flavivirus Protein C Differentially Affects Early RNA Synthesis and Growth in Mammalian and Arthropod Host Cells▽

Sabrina Schrauf,[1] Christian W. Mandl,[1]† Lesley Bell-Sakyi,[2] and Tim Skern[3]*

Institute of Virology, Medical University of Vienna, Kinderspitalgasse 15, A-1095 Vienna, Austria[1]; The Roslin Institute and Royal (Dick) School of Veterinary Studies, University of Edinburgh, Easter Bush Veterinary Centre, Roslin, Midlothian EH25 9RG, Scotland, United Kingdom[2]; and Max F. Perutz Laboratories, Medical University of Vienna, Dr. Bohr-Gasse 9/3, A-1030 Vienna, Austria[3]

Received 20 May 2009/Accepted 7 August 2009

The translation of flaviviral RNA genomes yields a single polyprotein that is processed into the mature proteins by viral and host cell proteases. Mature capsid protein C is freed from the polyprotein by the viral NS2B/3 protease, cleaving in the C-terminal region of protein C in front of the signal sequence for prM. Protein C has been shown to be involved in viral assembly and RNA packaging. To examine further the role of protein C and its production by proteolysis, we replaced the NS2B/3 capsid cleavage site in tick-borne encephalitis virus (TBEV) and West Nile virus (WNV) by the 2A protein of foot-and-mouth disease virus (TBEV-2A and WNV-2A). This obviated the need for NS2B/3 processing at the C terminus of mature protein C while simultaneously producing a 19-amino-acid extension on protein C. Infectious virions were generated with both viruses; the phenotype depended on the host cell. TBEV-2A replicated well in BHK-21 cells but was essentially incapable of replication in tick cells. In contrast, WNV-2A replicated well in mosquito cells but showed a small-plaque phenotype in Vero cells, with frequent production of larger plaques. Sequencing of viral RNA from the larger plaques showed substitutions in the signal sequence for prM, presumably improving coordinated protein processing at the C-prM junction. Furthermore, both TBEV-2A and WNV-2A were also defective in unpackaging and/or early RNA synthesis. Together, these results indicate a role for flavivirus protein C in both viral assembly and RNA replication, possibly by interacting with host cell factors required to set up the cell for RNA replication.

The genomes of single-stranded positive-sense RNA viruses are translated immediately on their release into the cytoplasm. The initial product of translation is mostly a single large polyprotein precursor that is proteolytically processed into the mature viral proteins. In this way, a number of proteins with distinct biochemical functions can be generated from limited genetic information. Processing strategies vary across viral families. Thus, the polyprotein of picornaviruses is exclusively processed by virus-encoded proteases (4, 20), whereas those of the family *Flaviviridae* require both virus-encoded and host cellular proteases (21). In members of the latter family, the polyprotein traverses the membranes of the endoplasmic reticulum (ER) several times, thus preventing access by the viral protease in the cytoplasm to the cleavage sites on the polyprotein parts inside the ER lumen. Cleavage at these sites is performed by the host signalase enzyme.

For productive infection, proteolytic processing and assembly of the virus particle from the structural proteins must be closely coordinated. In tick-borne encephalitis virus (TBEV) and West Nile virus (WNV), two important human pathogens of the genus *Flavivirus*, processing of the structural proteins C, prM, and E is strictly coupled (29). The viral NS2B/3 protease performs the first cleavage of the polyprotein, cleaving on the cytoplasmic side of the ER membrane to generate the mature capsid protein C (Fig. 1A) (1, 43). Only if this NS2B/3-induced cleavage has taken place can the host signalase enzyme inside the ER lumen gain access to its cleavage site at the N terminus of prM (22, 38). After these cleavages, prM and E remain anchored in the ER membrane, whereas the mature capsid protein C participates in RNA packaging and particle assembly with newly synthesized mRNA. Disturbance of these concerted cleavage events generally impairs (2, 23, 39) or even abrogates (19) virion production. Nevertheless, previous investigations of the C-terminal region of TBEV protein C revealed remarkable functional flexibility in the exact NS2B/3 cleavage position, as well as the cleavage substrate (35). In addition, several groups have also been able to supply protein C in *trans* to allow single-round infectious particles of several flaviviruses to be generated (10, 13, 27, 36, 40).

We wished to use this flexibility of the TBEV protein C to examine the effect on viral replication of the cleavage of C by an alternative *cis* processing mechanism, as well as the role of C itself. However, given the observed flexibility, it appeared necessary to add an appreciable number of amino acids to protein C to be sure that measurable effects on replication could be observed. Therefore, we decided to replace the NS2B/3 cleavage site between C and prM with the 2A protein sequence of foot-and-mouth disease virus (FMDV). This 20-amino-acid protein sequence contains a proline-glycine-proline sequence at its C terminus that causes ribosomes to skip the formation of a peptide bond at the C terminus of 2A without release of the ribosome. Thus, protein synthesis can

* Corresponding author. Mailing address: Max F. Perutz Laboratories, Medical University of Vienna, Dr. Bohr-Gasse 9/3, A-1030 Vienna, Austria. Phone: 43 1 4277 61620. Fax: 43 1 4277 9616. E-mail: timothy.skern@meduniwien.ac.at.

† Present address: Novartis Vaccines and Diagnostics, Inc., 350 Massachusetts Ave., Cambridge, MA 02139.

▽ Published ahead of print on 19 August 2009.

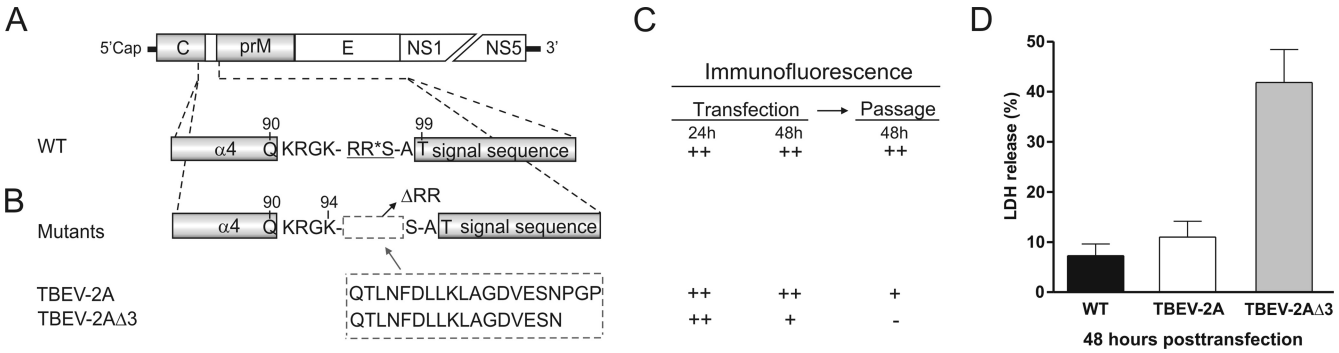

FIG. 1. Replication of WT TBEV, TBEV-2A, and TBEV-2AΔ3 in BHK-21 cells. (A) Schematic drawing of the WT TBEV genome, the C-terminal region of the capsid protein, and the signal sequence for prM (not drawn to scale). The NS2B/3 cleavage site is underlined, and the cleavage position is marked by an asterisk. The numbers at the top refer to the amino acid positions within protein C. (B) The engineered mutations are shown, together with the corresponding designations. (C) Results of immunofluorescence staining. BHK-21 cells were transfected with WT and mutant RNAs, and viral-protein expression was detected with a polyclonal serum 24 and 48 h posttransfection and 48 h after inoculation of fresh cells with supernatants derived from infected cells. ++, strong signal; +, weak signal; −, no signal. (D) Cytopathogenicity. The concentration of the enzyme LDH, released upon cell disintegration, was measured in the supernatants and standardized to the maximum LDH release as described in Materials and Methods.

continue on the same mRNA and translate a downstream coding sequence (3, 6, 8, 31).

This strategy enables the synthesis and release of C from prM from the same open reading frame without requiring any proteolytic activity. Simultaneously, a 19-amino-acid extension at the C terminus of protein C is generated, increasing the molecular mass of the protein (termed C-2A protein) by about 20%. With this system, we show that the FMDV 2A sequence can indeed replace the NS2B/3 cleavage site between the capsid protein C and the protein prM in both TBEV and WNV and allow production of infectious virions. TBEV-2A grew well in mammalian cells but extremely poorly in tick cells, whereas WNV-2A replicated well in insect cells but was genetically unstable in mammalian cells. As well as an influence on the assembly and physicochemical properties of the virions, we observed a distinct influence on early RNA synthesis, suggesting a previously unknown role of protein C in the early stages of this process that varies depending on the virus and the host cell.

MATERIALS AND METHODS

Cells and viruses. BHK-21 (ATCC CCL10) cells and the *Ixodes ricinus* embryo-derived cell line IRE/CTVM18 were cultured as described previously (5, 35). For the production of TBEV from IRE/CTVM18 cells, the culture medium was supplemented with 20 mM HEPES, pH 7.4, and 0.6% 1 N NaOH. Vero cells (ATCC CCL-81) were grown in Eagle's minimal essential medium supplemented with 10% fetal calf serum (FCS), 30 mM L-glutamine, 100 units/ml penicillin, and 1 μg/ml streptomycin. Infections were done in medium containing 2% FCS. For growth curve analysis, the medium was buffered with 15 mM HEPES, pH 7.4, and the FCS was replaced with 1% (wt/vol) bovine serum albumin. *Aedes albopictus* C6/36 cells were grown in Eagle's minimal essential medium (without $NaHCO_3$) supplemented with 10% FCS, 20 mM L-glutamine, 100 units/ml penicillin, 1 μg/ml streptomycin, 13 mM sodium hydroxide, 19 mM HEPES, pH 7.4, and 0.2% 50× tryptose-phosphate. For growth curve analysis, the FCS was reduced to 1%.

All genomic constructs used in this study were based on Western subtype TBEV strain Neudoerfl (GenBank accession no. U27495) (25) and WNV strain NY99 (GenBank accession no. FJ151394). The WNV strain (kindly provided by E. Gould and R. Shope) was isolated from a dead crow in New York in 1999 and passaged three times in Vero cells prior to RNA isolation and cDNA clone construction, as described elsewhere (34).

Mutant construction and in vitro RNA transcription and transfection. Plasmid pTNd/c contains a full-length genomic cDNA insert of wild-type (WT) TBEV strain Neudoerfl. Plasmid pTNd/5′ containing cDNA of the 5′ one-third of the genome was used to construct plasmid TBEV-2A/5′, which has the capsid NS2B/3 cleavage site (amino acids 95 to 96) replaced by the FMDV-2A sequence QTLNFDLLKLAGDVESNPGP. The deletion of the PGP motif was performed on plasmid TBEV-2A/5′ using the Gene Tailor site-directed mutagenesis system. Mutations were transferred into the full-length infectious cDNA clone pTNd/c by using two unique restriction sites (SalI and SnaBI).

Plasmids WNV-K1 and -K4, comprising the 5′ one-third and the 3′ two-thirds of the WT WNV genome, respectively, were used to generate infectious full-length RNA after in vitro ligation. To construct WNV-2A, amino acid 105 in the NS2B/3 cleavage site at the C terminus of protein C in plasmid WNV-K1 was replaced by the 2A sequence. For generation of WNV-2AΔ3, the PGP motif of plasmid WNV-K1-2A was deleted by site-directed mutagenesis. Full-length DNA templates were obtained by in vitro ligation of BstEII-digested 5′ and 3′ plasmids.

In vitro RNA transcription and transfection by electroporation were carried out as described previously (25, 35). To monitor RNA replication and RNA export following electroporation, BHK-21 cells were transfected with equimolar amounts of RNA (1.3×10^{12} RNA molecules), and the parameters were monitored by quantitative real-time PCR (qPCR) after reverse transcription of the viral RNA, as described previously (35).

Detection of viral proteins. The processing of the structural proteins was monitored as described previously (35) by immunoblotting using samples taken at the times indicated. Briefly, transfected cells disseminated in six-well plates were lysed 24 h posttransfection, and viral proteins were detected with a rabbit polyclonal anti-TBEV serum that recognized all three structural proteins (35) or with a polyclonal antibody directed against the WNV protein C (ProSci Inc.). Western blot analysis was also used to determine the virion composition of TBEV-2A. To this end, BHK-21 cells were transfected with TBEV-2A RNA; 48 h later, TBEV-2A particles in the cell culture supernatants were pelleted by ultracentrifugation. Then, the protein E concentration was determined by E-specific four-layer sodium dodecyl sulfate (SDS) enzyme-linked immunosorbent assay (ELISA) (12). Equal amounts (about 300 ng) of TBEV-2A and a gradient-purified WT virus control were loaded on a 15% polyacrylamide gel, and the viral proteins were separated under SDS denaturing conditions. Identification of viral structural proteins by immunoblotting was performed as described above.

Particle characterization. For determination of the buoyant density, BHK-21 cells were electroporated with TBEV-2A RNA, and virus particles were harvested 48 h postelectroporation. Then, the viral material was pelleted by ultracentrifugation and subjected to rate zonal and subsequent equilibrium density gradient centrifugation as described previously (9, 33). For the WT standard, WT TBEV (15 μg), previously purified using two cycles of sucrose gradient centrifugation as described elsewhere (11), was used. This was then also subjected to rate zonal and equilibrium density centrifugation. All gradients were fractionated

with a Piston Gradient Fractionator using downward displacement, and the protein E concentration in each fraction was measured by E-specific four-layer SDS ELISA (12). The RNA contents of protein E-containing fractions were further determined by qPCR following reverse transcription of the RNA as described in a previous study (35). The sucrose density of the peak fraction of the equilibrium density gradient was determined by precision weighing and by refractometry with an Abbé refractometer (Atago).

Multistep growth curves. For analysis of the growth properties of TBEV-2A, BHK-21 and IRE/CTVM18 cells grown in six-well plates were infected with WT TBEV and TBEV-2A stock preparations at a low multiplicity of infection (MOI) (0.01 for BHK-21 cells and 0.1 for IRE/CTVM18 cells unless otherwise stated). For analysis of intracellular RNA replication after infection, BHK-21 cells grown in 24-well plates were infected with WT TBEV and TBEV-2A at MOIs of 1 and 10. After 1 h, the cells were washed three times with medium containing 1% FCS. Then, cells were lysed at different time points (prior to commencement of a secondary round of replication), and cytoplasmic RNA was purified using an RNeasy Mini Kit and subjected to qPCR following reverse transcription of the RNA as described previously (17). For analysis of the growth properties and stability of WNV-2A, C6/36 and Vero cell monolayers in six-well plates were infected with WT WNV, WNV-2A, and WNV-2A revertant stock preparations at an MOI of 0.01. Aliquots of supernatants (500 μl) were taken at different time points, and virus titers and plaque morphology were determined by focus assay and plaque assay, respectively. For analysis of intracellular RNA replication after infection, Vero cells were grown in 24-well plates and infected with WT-WNV, WNV-2A, and WNV-2A-S120N (containing Asn at position 120 of the signal sequence of prM) at an MOI of 10. Then, cells were lysed at different time points, and intracellular RNA levels were determined as described above. Quantitation of the RNA was performed by qPCR following reverse transcription of the viral RNA as described elsewhere (34).

Focus and plaque assays. To quantify the production of infectious TBEV particles, immunochemical focus assays were performed (35). For quantification of WNV titers and determination of plaque morphologies, a plaque assay in Vero cells was carried out. Vero cell monolayers in 12-well plates were incubated for 1 h with serial dilutions of virus. Then, the cells were overlaid with growth medium containing 5% instead of 10% FCS and 0.3% agarose (Sigma). After an incubation period of 4 to 5 days, the cells were fixed and stained with a solution of 4% formaldehyde and 0.1% crystal violet.

Cytotoxicity assay. To determine the cytopathic effect (CPE), a cytotoxicity assay was performed. To this end, equimolar amounts of RNAs were transfected into BHK-21 cells, and the concentration of the enzyme lactate dehydrogenase (LDH) released from disintegrating cells was quantified spectrophotometrically using a commercially available cytotoxicity assay (Promega). To determine the maximum LDH release, cells were lysed completely by several freeze-thaw cycles. The observed absorbance values were standardized using the following formula: (experimental release − mock release)/(maximal release − mock release) × 100%.

RESULTS

The FMDV 2A protein sequence can replace the NS2B/3 cleavage site at the C terminus of protein C in TBEV. Several groups have shown that protein C of various members of the flavivirus family can be supplied in *trans*. We wished to investigate the situation when protein C is present on the same polyprotein molecule but not generated by NS2B/3 cleavage. To this end, we deleted the functionally relevant NS2B/3 cleavage motif in a full-length TBEV clone and replaced it with the 20-amino-acid FMDV 2A protein sequence (TBEV-2A) (Fig. 1A and B). The presence of this sequence in the TBEV polyprotein should have resulted in immediate formation of the mature capsid protein during polyprotein synthesis independently of the NS2B/3 protease. If this were the case, the C terminus of protein C should possess a 19-amino-acid 2A extension and allow us to investigate the effect of such an extension. In contrast, the N terminus of prM should remain unaffected, as it is generated by the host signalase cleaving at the C-prM junction inside the ER lumen.

We first examined the ability of TBEV-2A to replicate and translate proteins in BHK-21 cells. To this end, WT TBEV and TBEV-2A RNAs were transcribed in vitro and introduced into cells by electroporation. Intracellular protein E expression was used as a measure of replication and translation, as it had been shown that only replication-competent mutants produced enough viral proteins to be detectable via immunofluorescence (16). Following staining with an antiserum predominantly recognizing protein E, cells transfected with WT or mutant RNA exhibited protein E expression both 24 and 48 h posttransfection (Fig. 1C), indicating that TBEV-2A could perform both RNA replication and translation.

We also examined the effect of deleting the essential PGP in the FMDV 2A sequence of TBEV-2A (TBEV-2AΔ3) (Fig. 1B and C). Protein expression from this RNA could be detected 24 h posttransfection, revealing that the input RNA from TBEV-2AΔ3 can also be translated and replicated. However, inspection of the cells by phase-contrast microscopy revealed that, in contrast to cells transfected with WT TBEV or TBEV-2A, most positive cells showed a strong CPE and subsequently died (data not shown). As a consequence, only 5 to 10% of the transfected cells expressed viral proteins 48 h posttransfection. To quantify the extent of the cytopathogenicity, equimolar amounts of RNAs were introduced into BHK-21 cells by electroporation, and the release of LDH from disintegrating cells was measured in the supernatants. At 48 h posttransfection, TBEV-2AΔ3 clearly caused a stronger LDH release than the WT and TBEV-2A (Fig. 1D). These results thus agree well with the observations from phase-contrast microscopy. Previously, we had observed that the production of severe CPEs by TBEV mutants was related to deficiencies in the processing of capsid protein C (35). The occurrence of this phenomenon with TBEV-2AΔ3 therefore strongly implied that the inactivation of the FMDV 2A sequence had interfered with coordinated protein processing, leading to the production of unprocessed proteins that caused CPE and cell death.

We therefore set out to examine polyprotein processing in WT TBEV and the two mutants constructed as described above. BHK-21 cells were transfected with WT and mutant RNAs, and cells were lysed 24 h posttransfection. To analyze the extent of cleavages at the C-prM junction, the viral structural proteins were detected using a polyclonal serum raised against TBEV particles (Fig. 2A). WT TBEV exhibited prominent bands for the three structural proteins E, prM, and C (Fig. 2A, lane 4). TBEV-2A also showed distinct protein E and prM bands (Fig. 2A, lane 2); however, the C protein was not visible. Instead, a new band was now visible, corresponding in size to the C-2A protein (Fig. 2A, lane 2). The presence of this C-2A protein indicated that the FMDV 2A sequence was responsible for generating the mature protein C, as the protein would be smaller if additional cleavage by NS2B/3 had occurred.

In contrast, the mobility of prM did not change in TBEV-2A (Fig. 2A, lane 2). This indicated that the presence of the FMDV 2A protein did not qualitatively affect processing by the host signalase at the C terminus of the prM signal sequence.

We next analyzed the processing of the TBEV-2AΔ3 mutant (Fig. 2A, lane 3). In contrast to WT TBEV and TBEV-2A, TBEV-2AΔ3 showed only a distinct band corresponding to the E protein. In place of the other structural proteins, it exhibited a protein band corresponding to the C-2A–prM precursor.

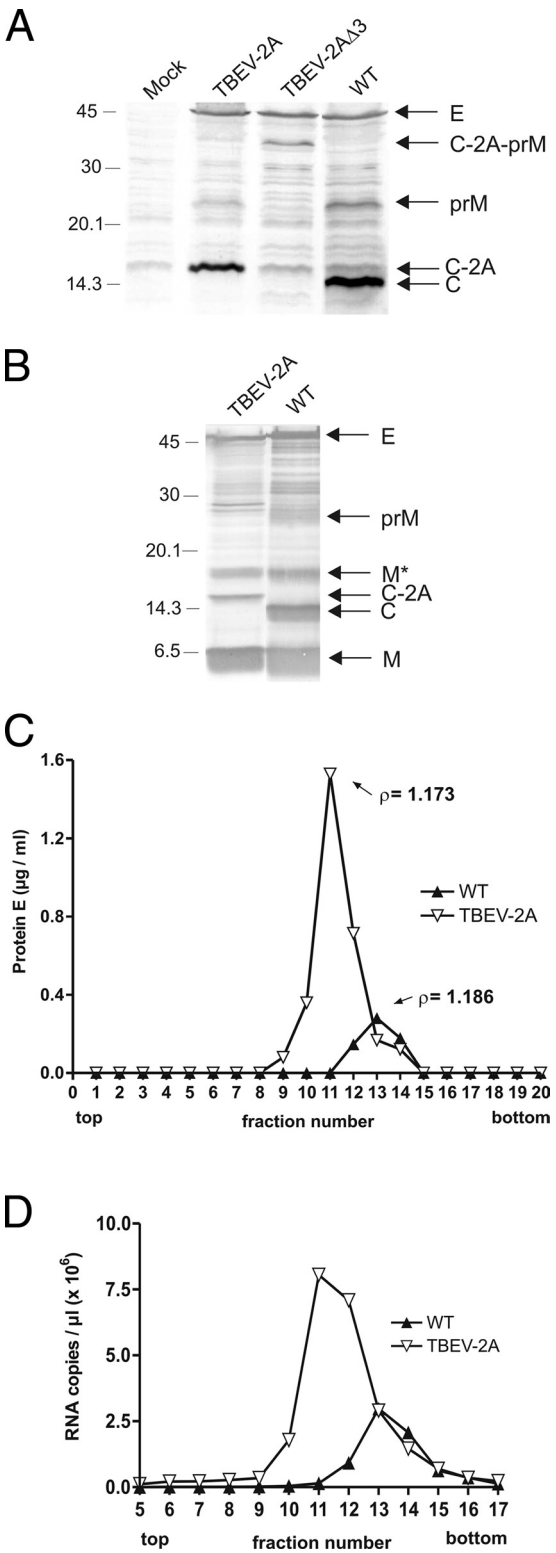

FIG. 2. Analysis of structural-protein processing (A) and secreted particles (B to D). (A) Cells transfected with WT or mutant RNAs were lysed 24 h posttransfection, and proteins were detected by immunoblotting using a rabbit polyclonal serum against the TBEV structural proteins. (B) Cells were transfected with TBEV-2A RNA; 48 h posttransfection, the components of particles secreted from the cells were compared to those of a WT preparation by immunoblotting using the same antiserum as in panel A. The WT preparation was selected because it contained an unusually high percentage (15%) of immature virus and thus a substantial amount of prM, enabling the identification of the protein. The positions of the structural proteins E, prM, M, C, and C-2A and the uncleaved precursor protein C-2A–prM are marked on the right, those of marker proteins in kDa on the left. The M* band is thought to be an "M-dimer," as described elsewhere, as it was previously shown by direct amino-terminal sequence analysis to contain protein M (37). (Panels A and B were edited with Adobe Photoshop to change the order of the lanes and to exclude unrelated samples.) (C and D) Cells were transfected with TBEV-2A RNA; 48 h posttransfection, particles were subjected to rate zonal and equilibrium density ultracentrifugation, and their protein E (C) and RNA (D) contents were determined as described in Materials and Methods. Virus purified by the same ultracentrifugation protocol was used as a control. The buoyant densities of the particles are indicated in panel C.

This indicated that the deletion of the PGP motif indeed abolished the generation of the mature capsid protein and disturbed the coordinated protein processing at the C-prM junction. The protein band that ran with the same mobility as the C-2A protein for TBEV-2AΔ3 corresponded to a nonspecific cellular protein, as it was also present at the same intensity in the mock-transfected and WT TBEV lanes.

TBEV-2A forms infectious virions independently of NS2B/3 cleavage in the C-terminal region of protein C. The above-described results implied that TBEV-2A should produce infectious viral progeny whereas the TBEV-2AΔ3 mutant would not. To examine this hypothesis, passaging experiments in BHK-21 cells were performed. Supernatants harvested 6 days after the transfection of cells with WT or mutant RNAs were transferred onto fresh BHK-21 cells, and protein E expression was again visualized by immunofluorescence staining 48 h postinfection (Fig. 1C). TBEV-2A yielded positive immunofluorescence staining, indicating that it had productively infected the BHK-21 cells. In contrast, no signal was observed with the TBEV-2AΔ3 deletion mutant. Due to the absence of both the NS2B/3 cleavage site and the PGP motif, no maturation of protein C occurred, and therefore, no infectious particles were generated. This result supports the view that the FMDV 2A protein sequence and not the NS2B/3 protease is responsible for polyprotein processing at the C terminus of protein C. Furthermore, a TBEV mutant can still produce infectious progeny despite the presence of a 19-amino-acid extension to protein C.

To exclude the possibility that sequence changes that might be responsible for the infectious phenotype had occurred in the course of the passaging experiments, viral RNAs were isolated 3 days postinfection after the first passage, and the entire structural-protein-coding region was sequenced following reverse transcription-PCR. No adaptive mutations were found. We also tried to select for spontaneous mutations in TBEV-2A by performing six serial passages. However, the only amino acid change detected was in protein E (threonine 310 to lysine), which presumably increased the affinity for heparan sulfate (data not shown) as observed previously (18, 26).

The above-mentioned experiments indicated that the infectious virus particles of TBEV-2A had incorporated C-2A in place of protein C. To confirm this, virus particles in supernatants from BHK-21 cells transfected with TBEV-2A RNA were pelleted by ultracentrifugation 2 days postelectroporation

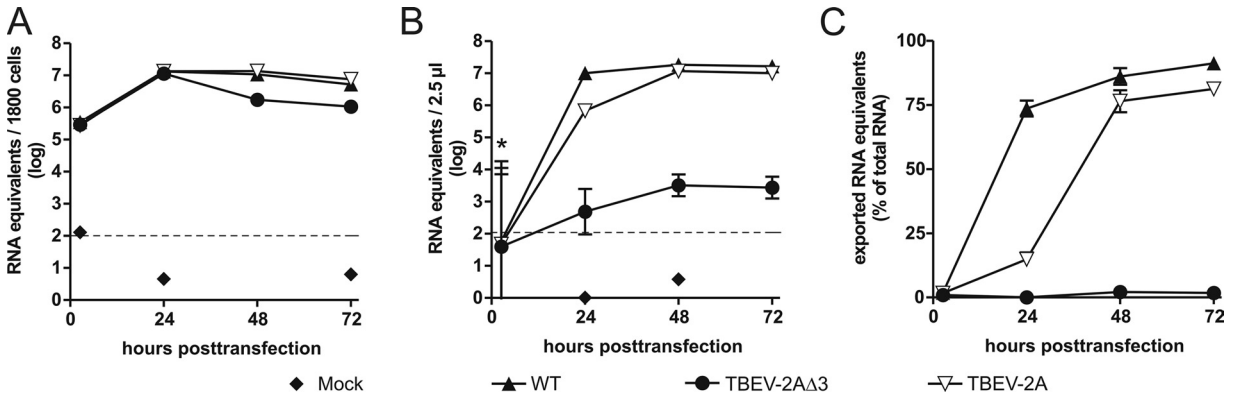

FIG. 3. RNA replication and export of TBEV-2A after electroporation. Shown are time course analyses of TBEV-2A after transfection of BHK-21 cells with equimolar levels of RNA. (A and B) Monitoring of RNA replication and RNA export by measuring intracellular (A) and extracellular (B) RNA amounts by qPCR following reverse transcription. (C) Analysis of RNA export efficiencies. The percentages of total RNA released into the supernatants were calculated from the intra- and extracellular RNA concentrations. All data points represent geometric mean values from two independent experiments. The error bars indicate the standard deviations. Inocula that were not completely removed by the washing steps are indicated by an asterisk. The values obtained for mock-transfected cells were below the cutoff (dashed lines).

and subjected to SDS-polyacrylamide gel electrophoresis to visualize the individual protein components (Fig. 2B). As a standard, gradient-purified WT virus particles were used. This virion preparation consisted of both mature and immature (at about 15%) particles to provide further insight into the maturation state of TBEV-2A particles. As expected, the WT virion preparation exhibited distinct bands for the three structural proteins E, C, and M and a minor band corresponding to the prM precursor protein. Particles of mutant TBEV-2A also showed prominent bands for proteins E and M; however, they showed no band for the C protein. Instead, these particles contained the C-2A protein observed in the cell lysates shown in Fig. 2A. In addition, no prM band was visible, indicating that the mutant TBEV-2A produced predominantly mature virus particles.

To characterize the particles further, we analyzed their buoyant densities. Again, supernatants from BHK-21 cells transfected with TBEV-2A RNA were subjected to ultracentrifugation 48 h postelectroporation to collect virus material, and the virus particles were then purified by rate zonal centrifugation followed by equilibrium density gradient centrifugation. As a standard, 15 μg of gradient-purified WT virus preparation was used. Figure 2C shows that the TBEV-2A particles had a somewhat lower buoyant density than the WT virions, indicating an influence of the C-2A protein on the virion structure.

To exclude the possibility that the observed lower buoyant density resulted from RNA-less virus particles, RNA was isolated from sucrose fractions in which protein E levels were measurable and subsequently determined by qPCR. As shown in Fig. 2D, we observed a picture with the RNA levels similar to that which we observed with the determination of the protein E levels. The RNA of TBEV-2A and the WT reached their peaks in the same fractions as the respective protein E concentrations. This further suggested the presence of RNA in the particles and, consequently, their integrity.

Taken together, these results indicate that a TBEV mutant with the FMDV 2A protein sequence instead of the NS2B/3 capsid cleavage site is able to produce infectious progeny consisting of proteins E, prM, and C-2A without any additional sequence adaptations. However, the lower buoyant density of the mutant particles indicates a structural difference of the mutant virions, suggesting an impact of the C-2A protein on the assembled virions.

The FMDV extension to protein C impairs the infectivity of TBEV-2A. The above-described experiments showed that the composition of TBEV-2A virions was similar to that of the WT virions but that they had a lower density. Next, we wanted to assess quantitatively the impact of the 19-amino-acid 2A extension of protein C in TBEV-2A on the replication, packaging, and export of viral RNA following introduction of the in vitro-synthesized RNAs into the cells by electroporation. TBEV-2AΔ3, shown above to be defective in virion production, was used as a negative control. First, BHK-21 cells were electroporated with equimolar amounts of WT TBEV, TBEV-2A, and TBEV-2AΔ3 RNAs. Then, the intracellular and extracellular viral-RNA levels were monitored by qPCR following reverse transcription over a period of 72 h (Fig. 3). As shown in Fig. 3A, the intracellular RNA concentrations of TBEV-2A and the WT were essentially the same, indicating that the RNA replication was not affected by the presence of the 2A sequence when the RNA was introduced into cells by electroporation. In contrast to TBEV-2A, the RNA levels of TBEV-2AΔ3 decreased at later time points, presumably due to the strong CPE and cell death observed with the mutant.

Analysis of the extracellular RNA levels, however, revealed differences between TBEV-2A and the WT at early time points (Fig. 3B). TBEV-2A showed a delay in the export of viral RNA, indicating a deficiency in RNA packaging. At later time points, however, the export of TBEV-2A RNA approached WT values (Fig. 3B). In contrast, the levels of RNA exported by TBEV-2AΔ3 remained low and were comparable to those measured previously using a packaging-deficient TBEV replicon mutant (35). These observations were strengthened by calculation of the percentages of RNA equivalents exported from infected cells by TBEV, TBEV-2A, and TBEV-2AΔ3 (Fig. 3C). Export of TBEV-2A was severely delayed at 24 h but recovered to almost WT levels at 48 h. Figure 3C also clearly

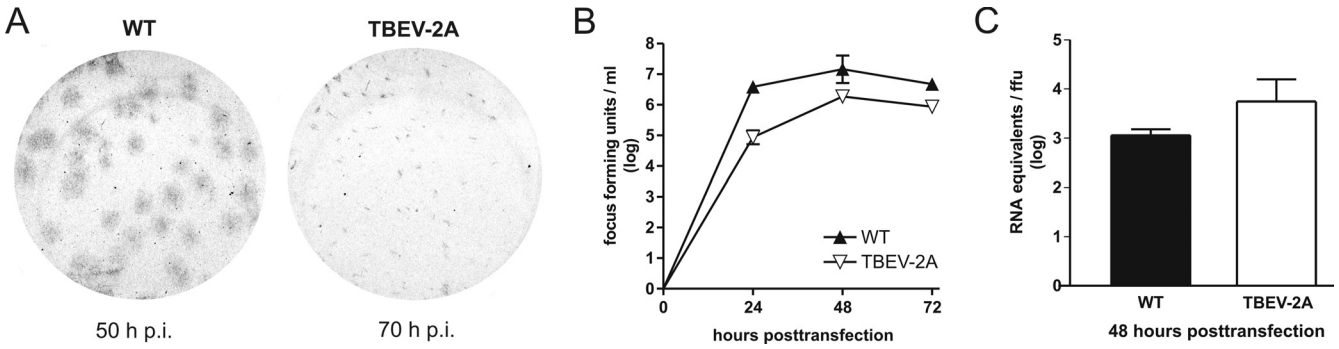

FIG. 4. Spread and infectious-virion production by TBEV-2A after electroporation. (A and B) Focus morphology (A) and infectivity titers (B) were determined using a focus-forming assay. (C) Specific-infectivity determination. The ratio of RNA equivalents per infectious unit was calculated for the 48-h time point. All data points represent geometric mean values from two independent experiments. The error bars indicate the standard deviations.

illustrates that the vast majority of the RNA produced by TBEV-2AΔ3 remained intracellular. The small amount of RNA found in the supernatant was due to the extensive levels of cell death.

To assess differences in the production of infectious virus progeny, the infectivity titers of WT and TBEV-2A virions were determined by examining their abilities to form foci in BHK-21 cells. Figure 4A shows that the foci formed by TBEV-2A were 5 to 10 times smaller than those observed with the WT. Furthermore, the foci of TBEV-2A could be visualized only at 70 h postinfection; WT foci could be visualized 50 h postinfection. These properties of the TBEV-2A foci clearly indicate a defect in viral spread. Determination of the number of foci produced at each time point confirmed that the efficiency of replication of TBEV-2A was reduced compared to the WT (Fig. 4B). After 24 h, the titer of TBEV-2A was 2.5 log units lower than that of the WT; 24 h later, the titer of TBEV-2A was still 1 log unit lower. Calculation of the specific infectivities (the ratio of RNA equivalents per infectious unit after 48 h) of the WT and TBEV-2A confirmed that TBEV-2A showed a small but significant loss of infectivity (Fig. 4C).

In summary, the presence of the 19-amino-acid 2A extension at the C terminus of protein C clearly affects the infectivity of the viral progeny.

Investigation of the replication of TBEV-2A in BHK-21 cells and in natural tick vector cells. To confirm and better quantify these differences in infectivity, we decided to use a more sensitive method to compare the growth patterns of the WT and TBEV-2A. To this end, we performed multistep growth curves in BHK-21 cells at a low MOI of 0.01. The reduced infectivity noted above resulted in titers of TBEV-2A approximately 2.0 log units below those of the WT in BHK-21 cells (Fig. 5A). This result clearly strengthens the notion that the presence of the FMDV-2A sequence impairs the growth and spread of virus progeny in BHK-21 cells.

We also wished to examine whether the infectivity of TBEV-2A was reduced in cells derived from the natural vector of TBEV, *I. ricinus*. We therefore performed multistep growth curves in the tick cell line IRE/CTVM18. To take into account the observed lower infection rate of tick cells (30), it was necessary to use an MOI of 0.1 for both the WT and TBEV-2A. This represented a 10-fold-higher MOI than that employed with BHK-21 cells (Fig. 5A). Robust growth of the WT was observed in IRE/CTVM18 cells (Fig. 5B). In contrast, no growth of TBEV-2A was observed (Fig. 5B), and release of a small number of virions was observed only at days 5 and 6. Infection at an MOI of 1 resulted in the appearance of virions at day 4. By day 6, there was almost a 1.0-log-unit increase in their production (data not shown).

Taken together, these results show that the presence of the

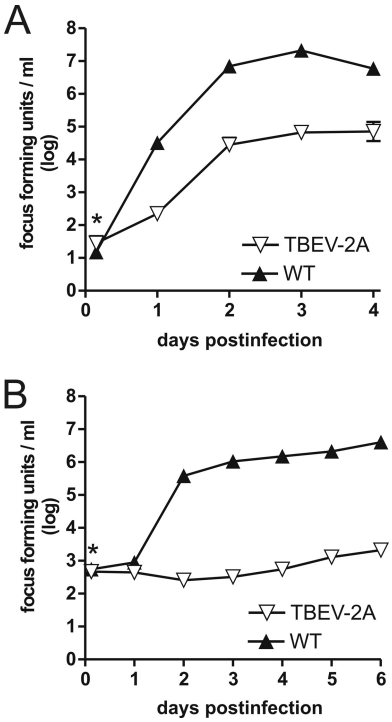

FIG. 5. Growth properties of TBEV-2A in BHK-21 (A) and IRE/CTVM18 (B) cells. The cells were infected at a low MOI (0.01 for BHK-21 cells and 0.1 for IRE/CTVM18 cells). Samples were taken at different time points, and the infectivity titers were determined using a focus assay. All data points represent geometric mean values from two independent experiments. The error bars indicate the standard deviations. Inocula that were not completely removed by the washing steps are indicated by asterisks.

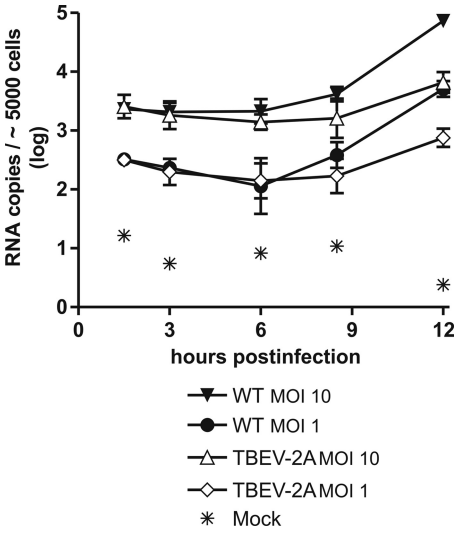

FIG. 6. RNA replication of TBEV-2A after infection of BHK-21 cells. The cells were infected at MOIs of 1 and 10. Samples were taken at different time points, and the intracellular RNA levels were measured. All data points represent geometric mean values from three independent experiments. The error bars indicate the standard deviations.

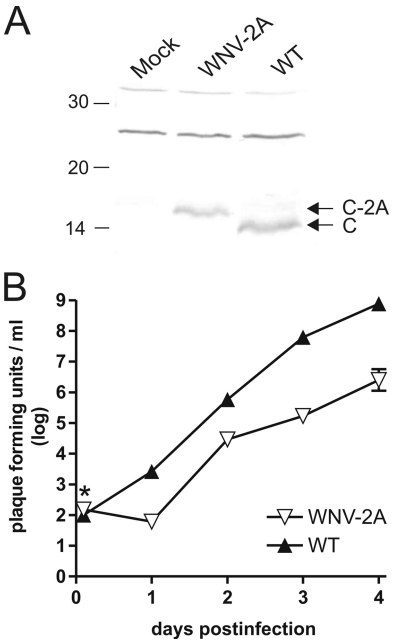

FIG. 7. Characterization of the WNV-2A mutant. (A) Western blot analysis of the capsid protein. Cells infected with WT WNV or WNV-2A were lysed 24 h postinfection, and the capsid protein was detected with a polyclonal antibody directed against protein C. The positions of the structural proteins C and C-2A are marked on the right, those of marker proteins in kDa on the left. (B) Growth curve analysis of WNV-2A in C6/36 cells. The cells were infected at an MOI of 0.01. Samples were taken at different time points, and the infectivity titers were determined using a plaque assay. All data points represent geometric mean values from two independent experiments. The error bars indicate the standard deviations. Inocula that were not completely removed by the washing steps are indicated by an asterisk.

FMDV 2A sequence in TBEV-2A impairs virus growth more strongly in the cells of the natural arthropod vector than in BHK-21 cells.

Early RNA synthesis is delayed upon infection with TBEV-2A. The experiments described above confirmed that TBEV-2A has a defect in infectivity and spread. To find the process or processes responsible, we examined intracellular RNA production in BHK-21 cells at time points prior to the commencement of a second round of infection. In contrast to the experiment shown in Fig. 3A, in which RNA replication had been studied after the introduction of RNA into cells by electroporation, we now wished to study early RNA replication upon infection with WT and mutant virions. Figure 6 shows that, at the 1-h time point, there was no difference between the WT and TBEV-2A. At the later times of 9 and 12 h, however, the number of RNA copies in the mutant was appreciably lower than with the WT. This was observed for both MOIs tested. This experiment indicates that the presence of the extended capsid protein in the infecting virion affects either uncoating or early RNA synthesis. This contrasts with the finding described above that the mutation did not affect RNA replication when RNA entered the cells by electroporation of naked RNA. We conclude, therefore, that the C-2A protein of the incoming virions interferes with unpackaging or early RNA synthesis, whereas de novo synthesis of C-2A in the presence of a large excess of naked RNA has no negative impact on RNA replication. The impaired infectivity and growth properties of the TBEV-2A virion may thus not only be caused by a defect in viral assembly, but also result to a significant degree from this impairment of unpackaging or early RNA synthesis.

One caveat to these experiments is that it may not be possible to detect early RNA replication above the background of input RNA after either electroporation or infection (Fig. 6). Thus, the possibility that the C-2A protein causes a delay in the synthesis of new positive strands from the double-strand replicative intermediate cannot be excluded.

Virion assembly of WNV can also occur independently of NS2B/3 capsid cleavage. The results show that a TBEV mutant with the FMDV 2A sequence in place of the NS2B/3 capsid cleavage site is able to produce infectious virus progeny, even though protein C has a 19-amino-acid extension. To investigate whether another flavivirus could also assemble virions with a C-2A protein, two analogous WNV mutants were generated, namely, mutant WNV-2A and mutant WNV-2AΔ3. First, the viability and infectivity of the mutants were determined by immunofluorescence staining after electroporation of RNAs into BHK-21 cells and after the first passage (data not shown). Both mutants were able to replicate their RNA and translate their proteins. Infectious particles were obtained with WT WNV and WNV-2A, but not with WNV-2AΔ3. Thus, this flavivirus can also form infectious virions containing the C-2A protein. To confirm the synthesis of the C-2A protein in WNV, cells were infected with WT and WNV-2A and lysed 24 h postinfection, and capsid proteins were detected by Western blotting. Figure 7A shows that WNV-2A exhibited a band corresponding in size to the C-2A protein.

In conclusion, these data demonstrate that the NS2B/3 capsid cleavage site of TBEV and WNV can in principle be replaced by the FMDV 2A sequence and lead to the production of infectious progeny in the two viruses.

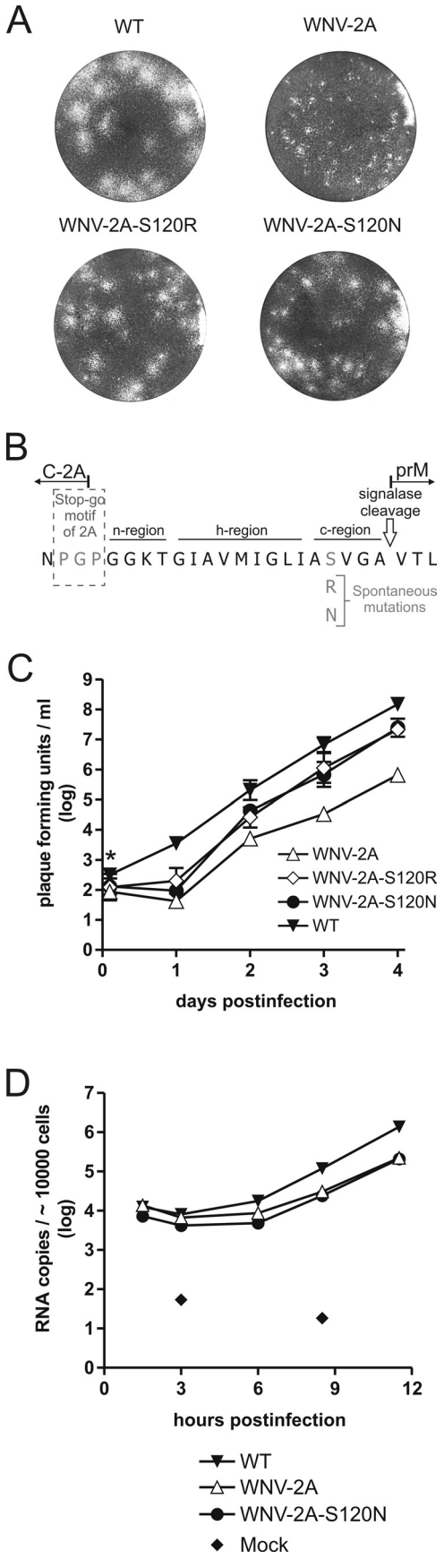

WNV-2A replicates well in mosquito cells but is unstable in Vero cells. We next assessed the impact of the FMDV 2A sequence on WNV growth and virion production by performing multistep growth curves at a low MOI (0.01). We first used C6/36 mosquito cells, derived from *A. albopictus*, which has been shown experimentally to be a competent vector of WNV (32). C6/36 cells were infected with WT WNV and WNV-2A, and virus production was measured by plaquing on Vero cells. These experiments revealed a distinct delay in viral-particle release by WNV-2A. Thus, 96 h postinfection, WNV-2A had reached titers of only 10^6 PFU per ml compared to $10^{8.5}$ for the WT (Fig. 7B). These data imply that the FMDV 2A extension to protein C interferes with, but does not abolish, growth of WNV in mosquito cells.

During the above-described experiment, we noticed that the plaques formed by WNV-2A were also smaller than those of the WT (Fig. 8A). Furthermore, while attempting to passage WNV-2A at low MOI in Vero cells to generate multistep growth curves, we frequently observed the spontaneous appearance of larger plaques between 2 and 4 days after transfection. Analysis by Western blotting of the state of the viral structural proteins from three independently isolated larger plaques showed that the C protein still possessed the 19-amino-acid extension (data not shown), indicating that the large-plaque phenotype did not derive from changes in the processing of the C protein. To find the mutations responsible for the large-plaque phenotype, we performed sequence analysis of the entire structural-protein-coding region of WNV-2A following reverse transcription-PCR of the three independently isolated larger plaques. In each case, the amino acid corresponding to serine 120 in the C terminus of the signal sequence for prM of the WT WNV sequence had been replaced by either arginine or asparagine (Fig. 8A and B). These two mutations were stable on two passages of the respective viruses for 4 days in both Vero and C6/36 cells. Multistep growth curves in C6/36 mosquito cells of plaque-purified WNV-2A containing these substitutions revealed a pattern of growth that was intermediate between those of WNV-2A and WT WNV (Fig. 8C).

To exclude the possibility that additional mutations were responsible for the revertant phenotype, we generated small

FIG. 8. Characterization of WNV-2A second-site revertants. (A) Plaque phenotype analysis of WT WNV, WNV-2A, and second-site revertants. Vero cells were infected with cell culture supernatants from the respective viruses. At 4 days postinfection, the cells were stained with crystal violet, and the plaque phenotypes were analyzed. (B) Acquired spontaneous mutations in the signal sequence for prM. The amino acid sequence around the WNV-2A C-prM junction is shown. The n, h, and c regions of the signal sequence for prM are indicated. (C) Growth curve analysis of the indicated viruses in C6/36 cells. The cells were infected at an MOI of 0.01. Samples were taken at different time points, and the infectivity titers were determined using a plaque assay. All data points represent geometric mean values from two independent experiments. The error bars indicate the standard deviations. Inocula that were not completely removed by the washing steps are indicated by an asterisk. (D) RNA replication of WT WNV, WNV-2A, and WNV-2A-S120N after infection of Vero cells. The cells were infected at an MOI of 10. Samples were taken at different time points, and the intracellular RNA levels were measured. All data points represent geometric mean values from two independent experiments.

PCR fragments containing the respective mutations and inserted the fragments into the genome of the original WNV-2A mutant. Viruses generated from such constructions showed the same large-plaque phenotype observed in the initial revertant WNV-2A viruses.

We also investigated the impact of the WNV C-2A protein on intracellular RNA replication at early time points after infection (Fig. 8D). Once again, the early RNA synthesis of the virus bearing the C-2A extension was delayed compared to the WT. Interestingly, this was also the case with the revertant. Once RNA replication had commenced with WNV-2A, however, it proceeded at the same rate as with the WT. This was in contrast to the situation with TBEV-2A, in which not only was early RNA synthesis delayed, but the rate of subsequent replication also appeared to be lower (compare Fig. 8D with Fig. 6). Further work will be necessary to show whether these differences are significant.

DISCUSSION

We have shown here that two flaviviruses in which the NS2B/3 cleavage site at the C terminus of protein C has been replaced by the 20-amino-acid sequence of the FMDV 2A protein can form infectious progeny. Nevertheless, replacement of the NS2B/3 cleavage site by the FMDV 2A sequence and the resulting extension of protein C resulted in the production of viruses with reduced efficiencies of replication. Unexpectedly, the extent of this reduction depended on the combination of virus and host system. Thus, TBEV-2A replication in BHK cells showed only slight reduction compared to that of the WT; however, the virus replicated extremely poorly in cells of the natural tick vector. In contrast, WNV-2A replicated almost at WT levels in cells of the natural mosquito vector but was unstable in Vero cells, and mutations in the signal sequence for prM in WNV-2A appeared rapidly.

What could be the reasons for the observed reduction in infectivity in TBEV-2A and WNV-2A and its dependency on the host cell employed? In these viruses, proteins C and prM are immediately separated; in the WT, this takes place only later, when NS2B/3 has already been synthesized. Thus, we showed that the NS2B/3 cleavage at the C terminus of protein C is not required when protein C is present on the same polyprotein as the other viral proteins. This is in good agreement with previous work that obviated the need for NS2B/3 cleavage of protein C by supplying protein C from separate translation units (10, 13, 27, 36, 40, 42). The viruses in such experiments replicated to high titers; therefore, it seems likely that interference with the NS2B/3 cleavage on protein C has only a minor effect on the efficiency of viral replication.

These findings imply that the reduced efficiency of replication of the two flaviviruses tested is most probably due to the impairment of the function of protein C by the 19-amino-acid 2A extension. For instance, the structural impact of the extension of protein C was reflected in the finding that TBEV-2A particles had lower buoyant density, indicating that the extension of protein C alters its arrangement in the particle or changes the packaging of the RNA. Unexpectedly, however, the extension to protein C also affected the early steps of RNA synthesis upon infection of cells by either TBEV-2A or WNV-2A, whereas RNA replication did not differ between the WT and the mutant when a high number of naked RNA molecules were introduced by electroporation. This suggests that the C-2A protein of the incoming virions impaired uncoating and/or early viral RNA synthesis, highlighting a previously undetected role of protein C in these processes. Given that TBEV-2A replicated extremely poorly in vector tick cells, it appears that this previously undetected role of protein C depends on the interaction with factors present in the host cell.

The observed defects in unpackaging and RNA replication must derive from the changes in the properties of the C terminus of protein C. Indeed, the 19-amino-acid 2A extension introduces 15 uncharged, mainly hydrophobic residues that may interfere with the known RNA binding ability of basic residues (14). Ma et al. (24) and Dokland et al. (7) have shown for protein C of dengue virus and WNV, respectively, that protein C occurs as a dimer with the two C-terminal helices lying close together and forming a broad interface for interaction with RNA. It seems possible that the 19-amino-acid 2A extension may interfere with the accessibility of the basic residues or hinder dimer formation, or both. These structural changes may be detrimental to the correct release of the RNA during uncoating or to the state of the RNA at the start of the replication process. Alternatively, the 2A sequences could affect the intracellular location of protein C during early RNA synthesis or its interaction with other components of the assembling replication complex. Notably, the C proteins of Kunjin virus and Japanese encephalitis virus have been shown to translocate to the nucleus during infection (28, 41).

A further indication that the effects of the 2A extension depend on the cell type infected was that revertant viruses were obtained with WNV-2A only when it was propagated in Vero cells. In these cells, WNV-2A showed a small-plaque phenotype, with larger plaques arising spontaneously. Reversion was due to replacement of the residue serine 120 of the WT WNV polyprotein by either arginine or asparagine. Surprisingly, however, Ser120 of the polyprotein does not lie at the site at which the FMDV 2A sequence separates proteins C and prM but in the C-terminal region of the signal sequence part for prM, just before the cleavage site of the signalase. Both mutations increase the overall polarity of the region, presumably increasing the efficiency of signalase cleavage at the N terminus of prM. The revertants are similar to those observed in WNV replicons in which protein C was provided in *trans* (42) in that the same amino acid, Ser120, was changed. However, Widman et al. found that in all the revertants, Ser120 had been replaced with cysteine. In our work, we twice observed asparagine and once arginine, but never cysteine. Furthermore, Widman et al. observed a frequent mutation in the cytoplasmic part of the signal sequence that we did not observe. This suggests that a different environment at, or different changes in, the NS2B/3 cleavage site requires different compensatory mutations in the signal peptide. In addition, a similar substitution in the signal sequence of TBEV has been found to release the dependency of signalase cleavage on the prior NS2B/3 cleavage of protein C (15, 19).

In summary, we have shown that both TBEV and WNV can produce infectious viral progeny when protein C is extended by 19 amino acids. However, the exact phenotype observed depended on the virus-host cell combination used. This implies

that the interactions between the viral protein C and cellular host factors are different in mammalian and arthropod cells.

ACKNOWLEDGMENTS

We thank Regina Kofler for her support in cultivation of the tick cells and Christian Taucher for critical reading.

This project was funded by the Austrian Science Fund, grant number FWF-P19528.

REFERENCES

1. **Amberg, S. M., A. Nestorowicz, D. W. McCourt, and C. M. Rice.** 1994. NS2B-3 proteinase-mediated processing in the yellow fever virus structural region: in vitro and in vivo studies. J. Virol. **68:**3794–3802.
2. **Amberg, S. M., and C. M. Rice.** 1999. Mutagenesis of the NS2B-NS3-mediated cleavage site in the flavivirus capsid protein demonstrates a requirement for coordinated processing. J. Virol. **73:**8083–8094.
3. **Atkins, J. F., N. M. Wills, G. Loughran, C. Y. Wu, K. Parsawar, M. D. Ryan, C. H. Wang, and C. C. Nelson.** 2007. A case for "StopGo": reprogramming translation to augment codon meaning of GGN by promoting unconventional termination (Stop) after addition of glycine and then allowing continued translation (Go). RNA **13:**803–810.
4. **Bedard, K. M., and B. L. Semler.** 2004. Regulation of picornavirus gene expression. Microbes Infect. **6:**702–713.
5. **Bell-Sakyi, L.** 2004. *Ehrlichia ruminantium* grows in cell lines from four ixodid tick genera. J. Comp. Pathol. **130:**285–293.
6. **de Felipe, P., L. E. Hughes, M. D. Ryan, and J. D. Brown.** 2003. Co-translational, intraribosomal cleavage of polypeptides by the foot-and-mouth disease virus 2A peptide. J. Biol. Chem. **278:**11441–11448.
7. **Dokland, T., M. Walsh, J. M. Mackenzie, A. A. Khromykh, K. H. Ee, and S. Wang.** 2004. West Nile virus core protein; tetramer structure and ribbon formation. Structure **12:**1157–1163.
8. **Donnelly, M. L., G. Luke, A. Mehrotra, X. Li, L. E. Hughes, D. Gani, and M. D. Ryan.** 2001. Analysis of the aphthovirus 2A/2B polyprotein 'cleavage' mechanism indicates not a proteolytic reaction, but a novel translational effect: a putative ribosomal 'skip.' J. Gen. Virol. **82:**1013–1025.
9. **Elshuber, S., S. L. Allison, F. X. Heinz, and C. W. Mandl.** 2003. Cleavage of protein prM is necessary for infection of BHK-21 cells by tick-borne encephalitis virus. J. Gen. Virol. **84:**183–191.
10. **Fayzulin, R., F. Scholle, O. Petrakova, I. Frolov, and P. W. Mason.** 2006. Evaluation of replicative capacity and genetic stability of West Nile virus replicons using highly efficient packaging cell lines. Virology **351:**196–209.
11. **Heinz, F. X., and C. Kunz.** 1981. Homogeneity of the structural glycoprotein from European isolates of tick-borne encephalitis virus: comparison with other flaviviruses. J. Gen. Virol. **57:**263–274.
12. **Heinz, F. X., K. Stiasny, G. Puschner-Auer, H. Holzmann, S. L. Allison, C. W. Mandl, and C. Kunz.** 1994. Structural changes and functional control of the tick-borne encephalitis virus glycoprotein E by the heterodimeric association with protein prM. Virology **198:**109–117.
13. **Khromykh, A. A., A. N. Varnavski, and E. G. Westaway.** 1998. Encapsidation of the flavivirus Kunjin replicon RNA by using a complementation system providing Kunjin virus structural proteins in *trans*. J. Virol. **72:**5967–5977.
14. **Khromykh, A. A., and E. G. Westaway.** 1996. RNA binding properties of core protein of the flavivirus Kunjin. Arch. Virol. **141:**685–699.
15. **Kofler, R. M., J. H. Aberle, S. W. Aberle, S. L. Allison, F. X. Heinz, and C. W. Mandl.** 2004. Mimicking live flavivirus immunization with a noninfectious RNA vaccine. Proc. Natl. Acad. Sci. USA **101:**1951–1956.
16. **Kofler, R. M., F. X. Heinz, and C. W. Mandl.** 2002. Capsid protein C of tick-borne encephalitis virus tolerates large internal deletions and is a favorable target for attenuation of virulence. J. Virol. **76:**3534–3543.
17. **Kofler, R. M., V. M. Hoenninger, C. Thurner, and C. W. Mandl.** 2006. Functional analysis of the tick-borne encephalitis virus cyclization elements indicates major differences between mosquito-borne and tick-borne flaviviruses. J. Virol. **80:**4099–4113.
18. **Kroschewski, H., S. L. Allison, F. X. Heinz, and C. W. Mandl.** 2003. Role of heparan sulfate for attachment and entry of tick-borne encephalitis virus. Virology **308:**92–100.
19. **Lee, E., C. E. Stocks, S. M. Amberg, C. M. Rice, and M. Lobigs.** 2000. Mutagenesis of the signal sequence of yellow fever virus prM protein: enhancement of signalase cleavage in vitro is lethal for virus production. J. Virol. **74:**24–32.
20. **Leong, L. C., C. T. Cornell, and B. L. Semler.** 2002. Processing determinants and functions of cleavage products of picornavirus polyprotein, p. 187–197. *In* B. L. Semler and E. Wimmer (ed.), Molecular biology of picornaviruses. ASM Press, Washington, DC.
21. **Lindenbach, B. D., H. J. Thiel, and C. M. Rice.** 2007. Flaviviridae: the viruses and their replication, p. 1101–1152. *In* D. M. Knipe and P. M. Howley (ed.), Fields virology. Lippincott Williams & Wilkins, Philadelphia, PA.
22. **Lobigs, M.** 1993. Flavivirus premembrane protein cleavage and spike heterodimer secretion require the function of the viral proteinase NS3. Proc. Natl. Acad. Sci. USA **90:**6218–6222.
23. **Lobigs, M., and E. Lee.** 2004. Inefficient signalase cleavage promotes efficient nucleocapsid incorporation into budding flavivirus membranes. J. Virol. **78:**178–186.
24. **Ma, L., C. T. Jones, T. D. Groesch, R. J. Kuhn, and C. B. Post.** 2004. Solution structure of dengue virus capsid protein reveals another fold. Proc. Natl. Acad. Sci. USA **101:**3414–3419.
25. **Mandl, C. W., M. Ecker, H. Holzmann, C. Kunz, and F. X. Heinz.** 1997. Infectious cDNA clones of tick-borne encephalitis virus European subtype prototypic strain Neudoerfl and high virulence strain Hypr. J. Gen. Virol. **78:**1049–1057.
26. **Mandl, C. W., H. Kroschewski, S. L. Allison, R. Kofler, H. Holzmann, T. Meixner, and F. X. Heinz.** 2001. Adaptation of tick-borne encephalitis virus to BHK-21 cells results in the formation of multiple heparan sulfate binding sites in the envelope protein and attenuation in vivo. J. Virol. **75:**5627–5637.
27. **Mason, P. W., A. V. Shustov, and I. Frolov.** 2006. Production and characterization of vaccines based on flaviviruses defective in replication. Virology **351:**432–443.
28. **Mori, Y., T. Okabayashi, T. Yamashita, Z. Zhao, T. Wakita, K. Yasui, F. Hasebe, M. Tadano, E. Konishi, K. Moriishi, and Y. Matsuura.** 2005. Nuclear localization of Japanese encephalitis virus core protein enhances viral replication. J. Virol. **79:**3448–3458.
29. **Mukhopadhyay, S., R. J. Kuhn, and M. G. Rossmann.** 2005. A structural perspective of the flavivirus life cycle. Nat. Rev. Microbiol. **3:**13–22.
30. **Ruzek, D., L. Bell-Sakyi, J. Kopecky, and L. Grubhoffer.** 2008. Growth of tick-borne encephalitis virus (European subtype) in cell lines from vector and non-vector ticks. Virus Res. **137:**142–146.
31. **Ryan, M. D., and J. Drew.** 1994. Foot-and-mouth disease virus 2A oligopeptide mediated cleavage of an artificial polyprotein. EMBO J. **13:**928–933.
32. **Sardelis, M. R., M. J. Turell, M. L. O'Guinn, R. G. Andre, and D. R. Roberts.** 2002. Vector competence of three North American strains of *Aedes albopictus* for West Nile virus. J. Am. Mosq. Control Assoc. **18:**284–289.
33. **Schalich, J., S. L. Allison, K. Stiasny, C. W. Mandl, C. Kunz, and F. X. Heinz.** 1996. Recombinant subviral particles from tick-borne encephalitis virus are fusogenic and provide a model system for studying flavivirus envelope glycoprotein functions. J. Virol. **70:**4549–4557.
34. **Schlick, P., C. Taucher, B. Schittl, J. L. Tran, R. M. Kofler, W. Schueler, A. von Gabain, A. Meinke, and C. W. Mandl.** 2009. Helices α2 and α3 of West Nile virus capsid protein are dispensable for assembly of infectious virions. J. Virol. **83:**5581–5591.
35. **Schrauf, S., P. Schlick, T. Skern, and C. W. Mandl.** 2008. Functional analysis of potential carboxy-terminal cleavage sites of tick-borne encephalitis virus capsid protein. J. Virol. **82:**2218–2229.
36. **Shustov, A. V., P. W. Mason, and I. Frolov.** 2007. Production of pseudoinfectious yellow fever virus with a two-component genome. J. Virol. **81:**11737–11748.
37. **Stadler, K., S. L. Allison, J. Schalich, and F. X. Heinz.** 1997. Proteolytic activation of tick-borne encephalitis virus by furin. J. Virol. **71:**8475–8481.
38. **Stocks, C. E., and M. Lobigs.** 1995. Posttranslational signal peptidase cleavage at the flavivirus C-prM junction in vitro. J. Virol. **69:**8123–8126.
39. **Stocks, C. E., and M. Lobigs.** 1998. Signal peptidase cleavage at the flavivirus C-prM junction: dependence on the viral NS2B-3 protease for efficient processing requires determinants in C, the signal peptide, and prM. J. Virol. **72:**2141–2149.
40. **Suzuki, R., E. R. Winkelmann, and P. W. Mason.** 2009. Construction and characterization of a single-cycle chimeric flavivirus vaccine candidate that protects mice against lethal challenge with dengue virus type 2. J. Virol. **83:**1870–1880.
41. **Westaway, E. G., A. A. Khromykh, M. T. Kenney, J. M. Mackenzie, and M. K. Jones.** 1997. Proteins C and NS4B of the flavivirus Kunjin translocate independently into the nucleus. Virology **234:**31–41.
42. **Widman, D. G., T. Ishikawa, R. Fayzulin, N. Bourne, and P. W. Mason.** 2008. Construction and characterization of a second-generation pseudoinfectious West Nile virus vaccine propagated using a new cultivation system. Vaccine **26:**2762–2771.
43. **Yamshchikov, V. F., and R. W. Compans.** 1994. Processing of the intracellular form of the west Nile virus capsid protein by the viral NS2B-NS3 protease: an in vitro study. J. Virol. **68:**5765–5771.